Progress In Electromagnetics Research M, Vol. 81, 75–84, 2019

Exact Analytical Method for Air-Gap Main Magnetic Field Computation and Cogging Torque of SMPM Motors

Libing Jing*, Junlin Chen, Zhangxian Huang, and Jun Gong

Abstract—This paper presents an exact analytical method to compute the air-gap magnetic field of surface-mounted permanent-magnet (SMPM) motors for evaluating slotting effects accurately. Solution field regions are divided into air-gap domain, permanent magnets (PM) domain, and slot domains. The Laplace's equations or Poisson's equations of the sub-domains are contacted by boundary conditions and then solved by exact analytical method. The actual height of slot and distance between slots are taken into account in the computation. Magnetic field distributions and cogging torque computed with the proposed analytical method are compared with those issued from 2-D finite-element method (FEM), and the comparison results are consistent and show the correctness and effectiveness of the proposed analytical method.

1. INTRODUCTION

Accurate knowledge of air-gap magnetic field distribution is necessary for the design of PM motors. The two-dimensional air-gap magnetic field of a surface-mounted permanent-magnet motor can be solved by numerical method or analytical method [1–5]. Although FEM has strong applicability and high computing precision, it takes a long time to model and calculate, so it is not convenient in the optimization design of motors. However, the physical concept of analytical method is clear, and the relationship between parameters and the distribution of magnetic field is more intuitively reflected by analytical function. The parameter adjustment is convenient; the calculation is little; and the speed is fast, which are beneficial to the optimal design and structural adjustment of the motor.

In the analysis of analytic model of motor, one of the most difficult tasks is how to accurately calculate the effect of slotting on air gap magnetic field. There are a lot of literatures about the application of analytical method to the calculation of air gap magnetic field of slotted motor [6–8]. References [9] and [10] adopte the scalar magnetic potentials method in polar coordinates to calculate the air-gap magnetic field of a surface-mounted permanent-magnet motor. Firstly, the air gap magnetic field of the motor without slots is calculated, and then the relative permeability function of the air gap is obtained by conformal transformation, which is multiplied by the air gap magnetic field without slots. Thus, the two-dimensional air gap magnetic field considering slotting effect is obtained. This method has the problem that the tangential magnetic field component of slot is hidden, which affects the accuracy of Maxwell stress tensor method in calculating electromagnetic torque. Reference [11] introduces plural relative permeance functions and overcomes the problem that the tangential component of magnetic field is hidden. However, the complex process in the solution of equation and the longer calculation time are not suitable for applications. The above methods adopt infinite slot model, without considering slotting effects and knowing magnetic conditions in the slots. It is not conducive to the accurate calculation of induction electromotive force of windings. In [12], an effective method to reduce the cogging torque of axial flux PM motors has been modeled. This method is curvature of the edges of magnets. This method

Received 4 April 2019, Accepted 22 May 2019, Scheduled 23 May 2019
* Corresponding author: Libing Jing (jinglibing163@163.com).
The authors are with the College of Electrical Engineering & New Energy, China Three Gorges University, Yichang 443002, China.

is modelled based on the idea of converting each pole to several sub-poles with different heights, widths, and air gap lengths. The results represent a reduction about 85% on the cogging torque amplitude and high accuracy of the suggested analytical model. The effect of the slots is also not taken into account.

According to the structure characteristics of the SMPM motor mode, the authors propose an analytical solution of the magnetic field distribution in the air gap of the SMPM motor. The analytical model is divided into three sub-domains in this paper, i.e., permanent magnet domains, air-gap domain, and slot domains. The Laplace's equation or Poisson's equation of the vector magnetic potential in each region is established. The sub-domain equation is connected by the boundary conditions. The analytical expressions of the no-load air gap magnetic field and the magnetic field in the slot are obtained by this method. Take an SMPM motor with 8-pole/12-slot as example; the cogging torque is calculated by the Maxwell stress method. Compared with the results gotten by FEM, the accuracy of calculation is guaranteed. This method is accurate and effective.

2. BASIC PRINCIPLES OF MAGNETIC FIELD CALCULATION

Take the inner rotor motor as an example. After slotting the stator core, it not only affects the distribution of the main magnetic field in the air gap, but also affects the adjacent slots. In order to simplify the problem, the following assumptions are made:

- End effects are neglected.
- Stator and rotor iron cores are infinitely permeable.
- Radially magnetized magnets with a relative recoil permeability.
- The stator slots have radial sides.

According to the structural characteristics of the motor and material property, the whole solution domain is divided into three parts: air-gap domain I, permanent magnet domain II, and slot domain $S_i\,(i = 1, 2, 3...Q)$. The motor physic model and its solution domain distribution in the 2-D polar coordinate system are shown in Fig. 1.

In Fig. 1, the geometrical parameters are the outer radius of the rotor yoke R_r, the outer radius of the permanent magnet R_m, the inner radius of the stator yoke R_s, and the outer radius of the slot-opening R_{sy}. The slot-opening angle is β, and θ_i is the mechanical position of the rotor.

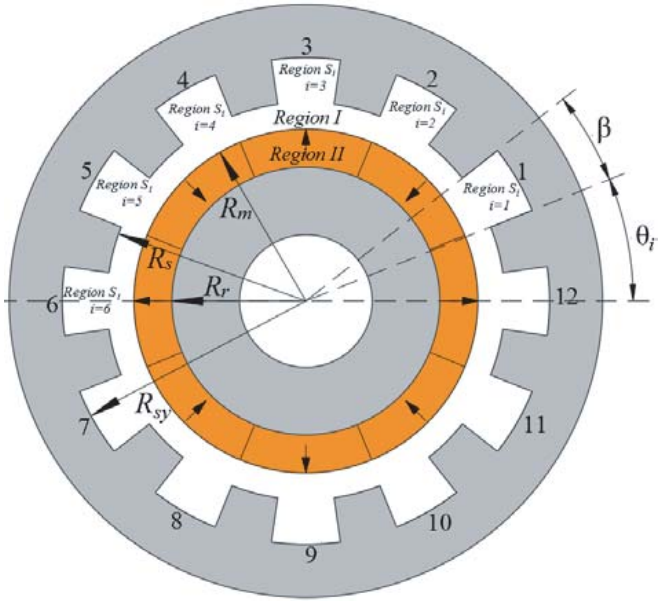

Figure 1. Geometry of an 8-pole/12-slot SMPM motor.

2.1. Mathematical Model of Air Gaps and PMs

In the 2-D polar coordinate, only Z axis has the virtual value when PM is radial magnetization. Its magnetization expression is r and θ function which is derived by the Fourier decomposition [1],

$$M(r,\theta) = \left[\sum_{v=1,3,5...}^{\infty} M_v \cos vp(\theta - \theta_0)\right] \vec{r} \tag{1}$$

with

$$M_v = 2(B_r/\mu_0)\alpha_p \frac{\sin(v\pi\alpha_p/2)}{v\pi\alpha_p/2} \tag{2}$$

where p is the number of pole pairs, α_p the pole-arc coefficient, and θ_0 the angular position between the PM and the standard position which is set originally.

In polar coordinates, the magnetic vector potential formulations of the air-gap domain I and the permanent magnet domain II are:

Laplace's equation of air-gap domain I:

$$\frac{\partial^2 A_I(r,\theta)}{\partial r^2} + \frac{1}{r}\frac{\partial A_I(r,\theta)}{\partial r} + \frac{1}{r}\frac{\partial^2 A_I(r,\theta)}{\partial \theta^2} = 0 \tag{3}$$

Poisson's equation of PM domain II:

$$\frac{\partial^2 A_{II}(r,\theta)}{\partial r^2} + \frac{1}{r}\frac{\partial A_{II}(r,\theta)}{\partial r} + \frac{1}{r^2}\frac{\partial^2 A_{II}(r,\theta)}{\partial \theta^2} = -u_r u_0 \nabla \times \vec{M} \tag{4}$$

with

$$\nabla \times \vec{M} = -\frac{1}{r}\frac{\partial M(r,\theta)}{\partial \theta} = \frac{1}{r}\sum_{v=1,3,5...}^{\infty} vpM_v \sin vp(\theta - \theta_0) \tag{5}$$

The general solution of Eqs. (3) and (4) can be shown as the following formulation by using the method of the separation of variables:

$$A_I(r,\theta) = \sum_{n=1}^{\infty}\left[(A_{In}r^{nm} + B_{In}r^{-nm})\cos(nm\theta) + (C_{In}r^{nm} + D_{In}r^{-nm})\sin(nm\theta)\right] \tag{6}$$

$$\begin{aligned} A_{II}(r,\theta) = {} & \sum_{n=1}^{\infty}\left[(A_{IIn}r^{nm} + B_{IIn}r^{-nm})\cos(nm\theta) + (C_{IIn}r^{nm} + D_{IIn}r^{-nm})\sin(nm\theta)\right] \\ & + \sum_{v=1,3,5...}^{\infty} \mu_0 r \frac{vp}{(vp)^2 - 1} M_v \sin(vp(\theta - \theta_0)) \end{aligned} \tag{7}$$

where m is the greatest common divisor of the number of slots and the number of poles.

The boundary conditions of the air-gap domain and PM domain are obtained according to electrical geometric model and material property:

$$\begin{cases} B_{\theta I}(r,\theta)|_{r=R_s} = -\left.\dfrac{\partial A_I}{\partial r}\right|_{r=R_s} = \begin{cases} -\left.\dfrac{\partial A_{si}}{\partial r}\right|_{r=R_s} & \theta_i \le \theta \le \theta_i + \beta \\ 0 & \text{elsewhere} \end{cases} \\ A_I(R_m,\theta) = A_{II}(R_m,\theta) \\ B_{\theta II}(r,\theta)|_{r=R_r} = -\left.\dfrac{\partial A_{II}}{\partial r}\right|_{r=R_r} = 0 \end{cases} \tag{8}$$

2.2. Mathematical Model of Slot Region

It is easy to get the solution of the Laplace equation by straight-slot model and simplify the boundary conditions of the slot domain. The magnetic vector potential formulation of the ith slot for no load is expressed as:

$$\frac{\partial^2 A_{si}(r,\theta)}{\partial r^2}+\frac{1}{r}\frac{\partial A_{si}(r,\theta)}{\partial r}+\frac{1}{r^2}\frac{\partial^2 A_{si}(r,\theta)}{\partial \theta^2}=0 \begin{cases} R_s \le r \le R_{sy} \\ \theta_i \le \theta \le \theta_i+\beta \end{cases} \tag{9}$$

where

$$\theta_i=-\frac{\beta}{2}+\frac{2i\pi}{Q} \tag{10}$$

The general solution of Eq. (9) can be shown as the following formulation by using the method of the separation of variables:

$$A_{si}(r,\theta)=A_0^i+\sum_{k=1}^{\infty}A_k^i\frac{\left(\frac{r}{R_{sy}}\right)^{k\pi/\beta}+\left(\frac{r}{R_{sy}}\right)^{-k\pi/\beta}}{\left(\frac{R_s}{R_{sy}}\right)^{k\pi/\beta}+\left(\frac{R_s}{R_{sy}}\right)^{-k\pi/\beta}}\cos\left(\frac{k\pi}{\beta}(\theta-\theta_i)\right) \tag{11}$$

with

$$A_0^i=\frac{1}{\beta}\int_{\theta_i}^{\theta_i+\beta}A_I(R_s,\theta)\cdot d\theta \tag{12}$$

$$A_k^i=\frac{2}{\beta}\int_{\theta_i}^{\theta_i+\beta}A_I(R_s,\theta)\cdot\cos\left(\frac{k\pi}{\beta}(\theta-\theta_i)\right)\cdot d\theta \tag{13}$$

where $k=1,2,3,...$ is the harmonic order in the slot domain.

The expression of the tangential flux density at the slot is derived from Eq. (11)

$$B_{\theta si}(R_s,\theta)=-\sum_{k=1}^{\infty}\alpha_k A_k^i\cos\left(\frac{k\pi}{\beta}(\theta-\theta_i)\right) \tag{14}$$

with

$$\alpha_k=\frac{k\pi}{\beta R_{sy}}\frac{\left(\frac{R_s}{R_{sy}}\right)^{k\pi/\beta-1}-\left(\frac{R_s}{R_{sy}}\right)^{-k\pi/\beta-1}}{\left(\frac{R_s}{R_{sy}}\right)^{k\pi/\beta}+\left(\frac{R_s}{R_{sy}}\right)^{-k\pi/\beta}} \tag{15}$$

where the boundary conditions of the slot domain are as follows:

$$\begin{cases} A_{si}(R_s,\theta)=A_I(R_s,\theta) \qquad \theta_i\le\theta\le\theta_i+\beta \\ B_{\theta si}(r,\theta)|_{r=R_{sy}}=-\left.\dfrac{\partial A_{si}}{\partial r}\right|_{r=R_{sy}}=0 \\ B_{rsi}(r,\theta)|_{\theta=\theta_i}=\left.\dfrac{1}{r}\dfrac{\partial A_{si}}{\partial \theta}\right|_{\theta=\theta_i}=0 \\ B_{rsi}(r,\theta)|_{\theta=\theta_i+\beta}=\left.\dfrac{1}{r}\dfrac{\partial A_{si}}{\partial \theta}\right|_{\theta=\theta_i+\beta}=0 \end{cases} \tag{16}$$

The magnetic vector potential formulations of the air-gap domain and the permanent magnet domain: A_{In}, B_{In}, C_{In}, D_{In} and A_{IIn}, B_{IIn}, C_{IIn}, D_{IIn} are derived from the above formulations (6), (7), (14) and the boundary conditions (8), (16). After getting the magnetic vector potential $A_I(r,\theta)$ of the air-gap domain, it can relieve the magnetic vector potential A_k^i (see Appendix A), then the magnetic field distribution is derived.

3. COGGING TORQUE

After slotting, the PM produces ripple torque that is not related to electricity. This torque is called the cogging torque. There are two methods to calculate the electromagnetic torque by the numerical method: The virtual displacement method and Maxwell stress method. Both methods can calculate the cogging torque. The virtual displacement method has deficiency of poor computational efficiency. If using Maxwell stress method, the result is independent of the integration path theoretically, because the calculation can be finished by integrating linearly along the circumference in the air-gap for only one time. Therefore, Maxwell stress method is used for calculating the cogging torque.

$$\begin{aligned} T_{cog} &= \frac{L_{ef}}{u_0}\int_0^{2\pi} r_e^2 B_{rI} B_{\theta I} d\theta = \frac{L_{ef} r_e^2}{u_0}\int_0^{2\pi} \sum_{n=1}^{\infty} \left[\begin{array}{l} -\left(A_{In} r^{nm-1} + B_{In} r^{-nm-1}\right) nm \sin nm\theta \\ +\left(C_{In} r^{nm-1} + D_{In} r^{-nm-1}\right) nm \cos nm\theta \end{array} \right] \\ &\quad \cdot \left(- \left[\begin{array}{l} \left(A_{In} r^{nm-1} - B_{In} r^{-nm-1}\right) nm \cos nm\theta \\ +\left(C_{In} r^{nm-1} - D_{In} r^{-nm-1}\right) nm \sin nm\theta \end{array} \right] \right) \cdot d\theta \\ &= \frac{2\pi L_{ef}}{u_0} \sum_{n=1}^{\infty} (nm)^2 [-A_{In} D_{In} + B_{In} C_{In}] \end{aligned} \tag{17}$$

According to Equation (17), the cogging torque can be gotten if getting the expression of magnetic vector potential $A_I(r, \theta)$ in air-gap domain.

4. ANALYTICAL RESULTS AND COMPARISON WITH FINITE ELEMENT CALCULATION

In order to verify the validity of this analytical method, the magnetic field and cogging torque of an inner-rotor motor with 8-pole/12-slot are calculated. Then the results are compared with those calculated by 2-D FEM. The main parameters of the motor are shown in Table 1.

Table 1. Main parameters of motor.

Parameter	value
Pole pairs	4
Number of slots	12
Inner radius of stator/mm	19
Slot open/mm	1.5
Height of slot/mm	15
Length of PM/mm	7.5
Pole-arc coefficient	1
Air gap length/mm	0.5
Remanence/T	1.0
Axial length/mm	10
Harmonic order in air-gap	200
Harmonic order in slotting	100

Figure 2 shows that the magnetic vector potential presents triangular waveform. Because of the slotting effect, the magnetic vector potential on the inner surface of the stator is not smooth. Therefore, it verifies the agreement between the calculated results of the program and those of the FEM.

Figure 3 shows the radial and tangential components of magnetic flux density waveforms for no-load condition in the middle of the air-gap (at $r = 18.75$ mm).

It can be seen from Fig. 3 that an excellent agreement with the results deduced from FEM is obtained.

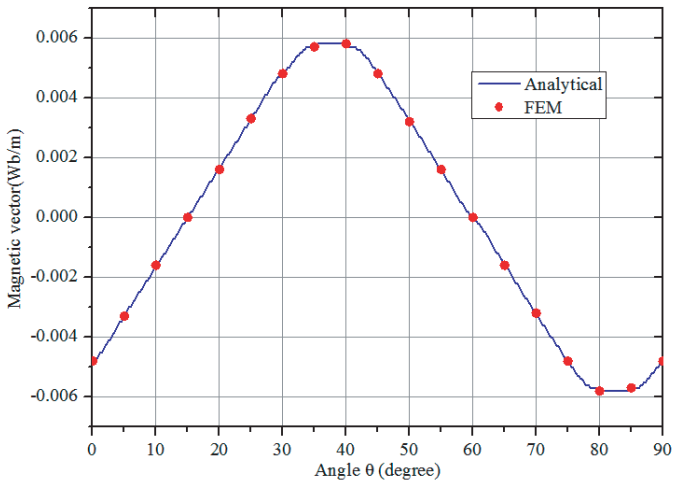

Figure 2. Magnetic vector potential distribution on the inner stator surface.

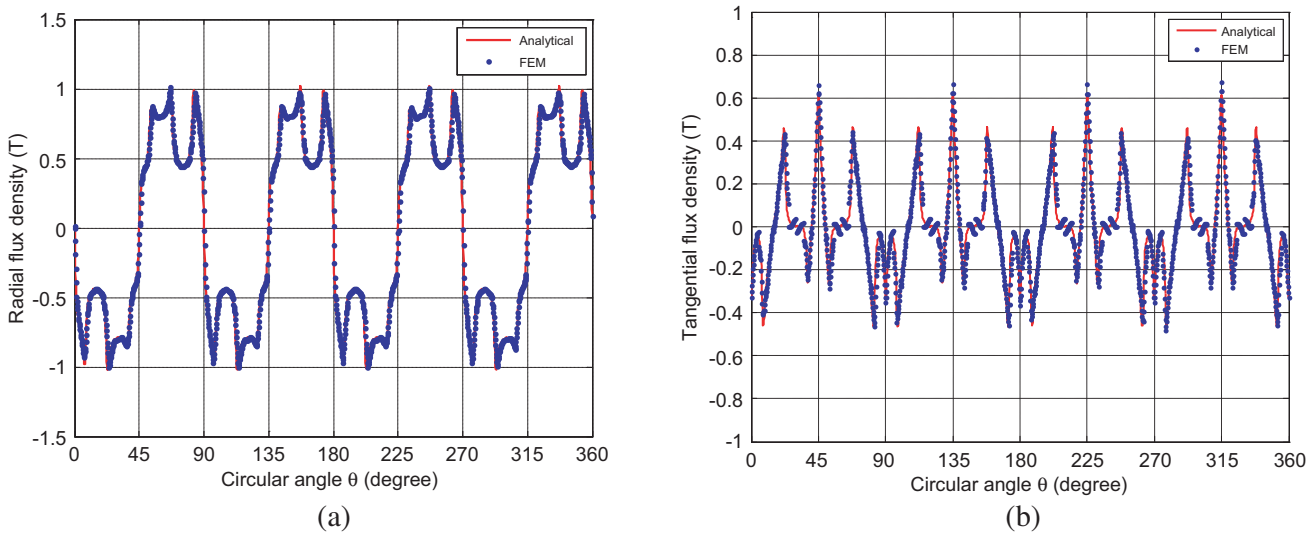

Figure 3. Flux density for no load condition in the middle of the air-gap. (a) Radial components of the flux density. (b) Tangential components of the flux density.

Figure 4 shows the cogging torque. The angular period of the cogging torque corresponds to the Least Common Multiple of $2p$ and Q giving $360°/\mathrm{LCM}(Q, 2p) = 15$. It can be seen that the proposed analytical model can predict the cogging torque with an excellent precision. It shows that the method is accurate and effective.

Figure 5 shows the tangential component of the air-gap flux density at $r = 19\,\mathrm{mm}$. Because of the discontinuity of the tangential component, the magnetic density amplitude at the edge of the teeth is larger; the center line of the slot is approximately zero; and the leakage of magnetic flux in the middle slot corresponding to the adjacent poles is larger. This is consistent with the calculation results of FEM, which proves the correctness of the calculation results and provides a basis for the subsequent calculation of conductor flux and induced potential in the slot area.

Figure 6 shows the electromagnetic torque waveforms. The machine is supplied with a three-phase sinusoidal current. It can be seen that the studied machine produces an average torque of 1.12 Nm. The torque ripples are due to the cogging torque but also to the space harmonics created by the stator winding distribution as well as the magnetization of the PMs. These ripples represent almost 18% of the average torque.

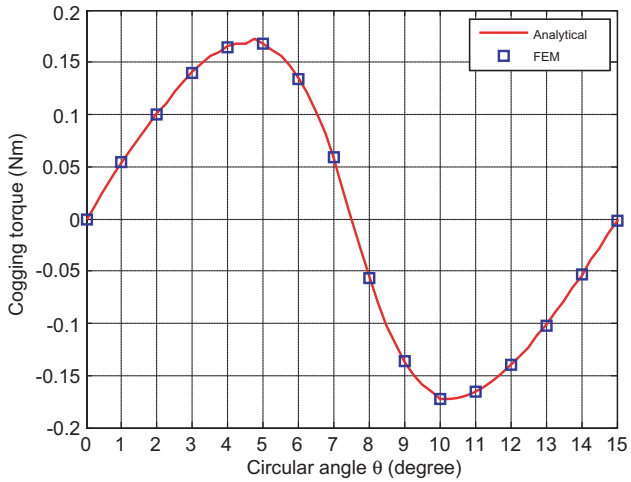

Figure 4. Cogging torque.

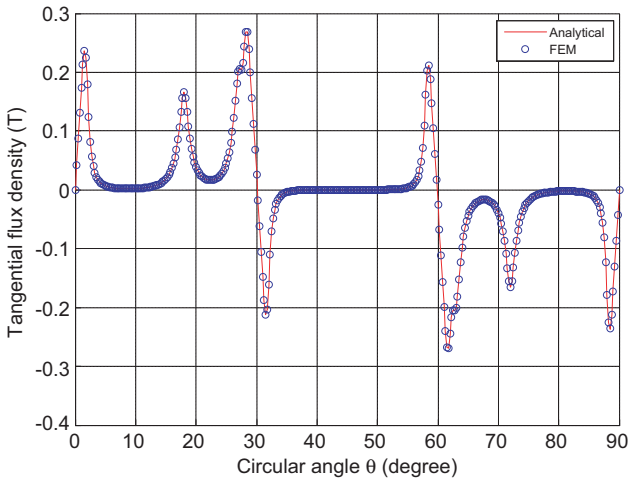

Figure 5. Tangential flux density waveform on the slot-opening.

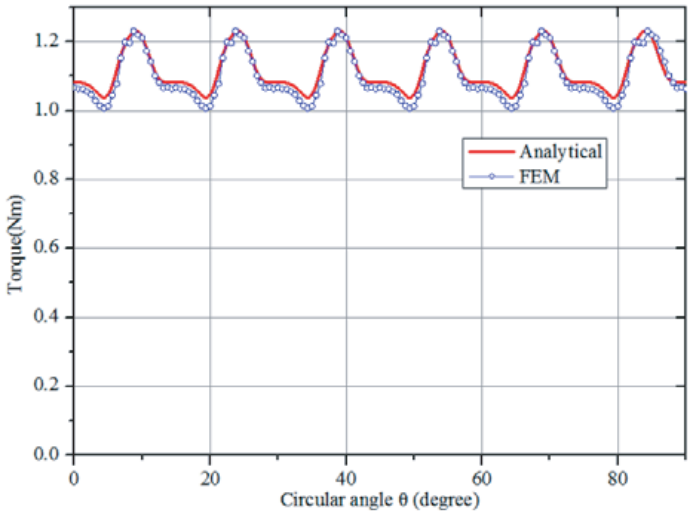

Figure 6. Electromagnetic torque.

5. CONCLUSION

In this paper, an exact analytical method for computing the air-gap field distribution in the SMPM motor with no-load magnetic vector potential considering slotting effects has been presented, and the corresponding calculation program is compiled. The main magnetic field of air-gap and the cogging torque are calculated. Compared with the results of FEM, the correctness and validity of this method are proved. This method not only ensures the accuracy of the calculation results, but also conveniently obtains the analytical solutions of the air gap magnetic field and the magnetic field in the slot. It provides convenience for further research on the physical quantities related to the air gap magnetic field and the magnetic field in the slot. The method adopted in this paper saves calculation speed, not only suitable for fractional slot motors, but also suitable for integer slot motors, and has universal applicability.

APPENDIX A.

A.1. Expressions of the Coefficients Air-Gap Domain I

$$\begin{aligned} A_{In} &= a_n\xi_n + \sin(vp\theta_0)\zeta_n \\ B_{In} &= a_n R_r^{2nm}\xi_n + \sin(vp\theta_0)R_s^{2nm}\zeta_n \\ C_{In} &= b_n\xi_n - \cos(vp\theta_0)\zeta_n \\ D_{In} &= b_n R_r^{2nm}\xi_n - \cos(vp\theta_0)R_s^{2nm}\zeta_n \end{aligned} \tag{A1}$$

PM domain II:

$$\begin{aligned} A_{IIn} &= a_n\xi_n + \sin(vp\theta_0)\eta_n \\ B_{IIn} &= a_n R_r^{2nm}\xi_n + \sin(vp\theta_0)\rho_n \\ C_{IIn} &= b_n\xi_n - \cos(vp\theta_0)\eta_n \\ D_{IIn} &= b_n R_r^{2nm}\xi_n - \cos(vp\theta_0)\rho_n \end{aligned} \tag{A2}$$

with

$$\xi_n = \frac{R_s^{nm}}{R_s^{2nm} - R_r^{2nm}} \tag{A3}$$

$$\zeta_n = \frac{u_0 M_n \left[-2R_r^{nm+1} - (nm-1)R_m^{nm+1} + (nm+1)\dfrac{R_r^{2nm}}{R_m^{nm-1}}\right]}{2((vp)^2-1)\left(R_s^{2nm} - R_r^{2nm}\right)} \tag{A4}$$

$$\eta_n = \frac{u_0 M_n \left[-2R_r^{nm+1} - (nm-1)R_m^{nm+1} + (nm+1)\dfrac{R_s^{2nm}}{R_m^{nm-1}}\right]}{2((vp)^2-1)\left(R_s^{2nm} - R_r^{2nm}\right)} \tag{A5}$$

$$\rho_n = \frac{u_0 M_n \left[-2R_r^{nm+1}R_s^{2nm} - (nm-1)R_m^{nm+1}R_r^{2nm} + (nm+1)\dfrac{(R_r R_s)^{2nm}}{R_m^{nm-1}}\right]}{2((vp)^2-1)\left(R_s^{2nm} - R_r^{2nm}\right)} \tag{A6}$$

$$a_n = \frac{2}{\tau}\frac{R_s}{nm}\sum_{i=1}^{Q}\sum_{k=1}^{\infty}\alpha_k A_k^i f_k^i(n) \tag{A7}$$

$$b_n = \frac{2}{\tau}\frac{R_s}{nm}\sum_{i=1}^{Q}\sum_{k=1}^{\infty}\alpha_k A_k^i g_k^i(n) \tag{A8}$$

$$f_k^i(n) = \int_{\theta_i}^{\theta_i+\beta}\cos\frac{k\pi}{\beta}(\theta-\theta_i)\cos nm\theta d\theta \tag{A9}$$

$$g_k^i(n) = \int_{\theta_i}^{\theta_i+\beta}\cos\frac{k\pi}{\beta}(\theta-\theta_i)\sin nm\theta d\theta \tag{A10}$$

- for $k\pi \neq n\beta$

$$\begin{cases} f_k^i(n) = \dfrac{-nm\beta^2\left[(-1)^k\sin nm(\beta+\theta_i) - \sin(nm\theta_i)\right]}{(k\pi)^2 - (nnm\beta)^2} \\ g_k^i(n) = \dfrac{nm\beta^2\left[(-1)^k\cos nm(\beta+\theta_i) - \cos(nm\theta_i)\right]}{(k\pi)^2 - (nnm\beta)^2} \end{cases} \tag{A11}$$

- for $k\pi = n\beta$

$$\begin{cases} f_k^i(n) = \dfrac{\beta}{2}\left[\cos(nm\theta_i) + \dfrac{1}{2k\pi}(\sin nm(\theta_i+2\beta) - \sin(nm\theta_i))\right] \\ g_k^i(n) = \dfrac{\beta}{2}\left[\sin(nm\theta_i) - \dfrac{1}{2k\pi}(\cos nm(\theta_i+2\beta) - \cos(nm\theta_i))\right] \end{cases} \tag{A12}$$

A.2. Expression of the Coefficient A_k^i for the ith Slot Domain

$$\begin{aligned} A_k^i &= \frac{2}{\beta}\int_{\theta_i}^{\theta_i+\beta} A_I(R_s,\theta)\cos\left(\frac{k\pi}{\beta}(\theta-\theta_i)\right)d\theta \\ &= \frac{2}{\beta}\int_{\theta_i}^{\theta_i+\beta}\sum_{n=1}^{\infty}\left[(A_{In}R_s^{nm}+A_{In}R_s^{-nm})\cos(nm\theta)+(C_{In}R_s^{nm}+D_{In}R_s^{-nm})\sin(nm\theta)\right] \\ &\quad \cdot\cos\left(\frac{k\pi}{\beta}(\theta-\theta_i)\right)d\theta \\ &= \frac{2}{\beta}\sum_{n=1}^{\infty}\left[\left(A_{In}R_s^{nm}+B_{In}R_s^{-nm}\right)f_k^i(n)+\left(C_{In}R_s^{nm}+D_{In}R_s^{-nm}\right)g_k^i(n)\right] \end{aligned} \tag{A13}$$

ACKNOWLEDGMENT

This work was supported by the National Natural Science Foundation of China (Project No. 51707072) and China Postdoctoral Science Foundation (Project No. 2018M632855).

REFERENCES

1. Noyal Doss, A., R. Brindha, K. Mohanraj, S. S. Dash, and K. M. Kavya, "A novel method for cogging torque reduction in permanent magnet brushless DC motor using T-shaped bifurcation in stator teeth," *Progress In Electromagnetics Research M*, Vol. 66, 99–107, 2018.
2. Onsal, M., B. Cumhur, Y. Demir, E. Yolacan, and M. Aydin, "Rotor design optimization of a new flux assisted consequent pole spoke-type permanent magnet torque motor for low-speed applications," *IEEE Trans. Magn.*, Vol. 54, No. 11, ID: 8206005, 2018.
3. Xie, K. F., D. W. Li, R. H. Qu, and D. Jiang, "Analysis and experimental comparison of spoke type and surface-mounted PM machines with fractional slot concentrated winding," *2016 19th International Conference on Electrical Machines and Systems (ICEMS)*, 1–6, 2016.
4. Zhou, Y., H. Li, and G. Meng, "Analytical calculation of magnetic field and cogging torque in surface-mounted permanent-magnet machines accounting for any eccentric rotor shape," *IEEE Trans. Ind. Electro.*, Vol. 62, No. 6, 3438–3447, 2015.
5. Zhao, N. N. and W. G. Liu, "Loss calculation and thermal analysis of surface-mounted PM motor and interior PM motor," *IEEE Trans. Magn.*, Vol. 51, No. 11, ID: 8112604, 2015.
6. Kumar, P., M. M. Reza, and R. K. Srivastava, "Analytical method for calculation of cogging torque reduction due to slot shifting in a dual stator dual rotor permanent magnet machine with semi-closed slots," *Progress In Electromagnetics Research M*, Vol. 70, 99–108, 2018.
7. Jing, L. B., R. H. Qu, W. B. Kong, D. Li, and H. L. Huang, "Genetic-algorithm-based analytical method of SMPM motors," *2017 IEEE International Electric Machines and Drives Conference (IEMDC),* 1–6, 2017.
8. Tiang, T. L., D. Ishak, C. P. Lim, and M. Rezal Mohamed, "Analytical method using virtual PM blocks to represent magnet segmentations in surface-mounted PM synchronous machines," *Progress In Electromagnetics Research B*, Vol. 76, 23–36, 2017.
9. Zhu, Z. Q., D. Howe, and E. Bolte, "Instantaneous magnetic field distribution in brushless permanent magnet DC motors, Part I: Open-circuit field," *IEEE Trans. Magn.*, Vol. 29, No. 1, 124–135, 1993.
10. Zhu, Z. Q. and D. Howe, "Instantaneous magnetic field distribution in brushless magnet DC motors, Part III: Effect of stator slotting," *IEEE Trans. Magn.*, Vol. 29, No. 1, 143–151, 1993.
11. Zarko, D., D. Ban, and A. L.Thomas, "Analytical calculation of magnetic field distribution in the slotted air gap of a surface permanent-magnet motor using complex relative air-gap permeance," *IEEE Trans. Magn.*, Vol. 42, No. 7, 1828–1837, 2006.

12. Pahlavani, M. A. and H. R. Gholinejad Omran, "A new analytical description and FEA validation of an effective method to reduce the cogging torque in SM-AFPM motors," *Progress In Electromagnetics Research M*, Vol. 42, 189–197, 2015.